Available online at www.sciencedirect.com
SCIENCE DIRECT
Biochemical and Biophysical Research Communications 347 (2006) 22–30
BBRC
www.elsevier.com/locate/ybbrc

DIXDC1 isoform, l-DIXDC1, is a novel filamentous actin-binding protein

Xianshu Wang [a], Li Zheng [a], Zhaozhu Zeng [a], Guangjin Zhou [a], Jeremy Chien [a], Chiping Qian [a], George Vasmatzis [a], Viji Shridhar [a], Lin Chen [b], Wanguo Liu [a,*]

[a] *Department of Laboratory Medicine and Pathology, Mayo Clinic/Mayo Medical School, Rochester, MN 55905, USA*
[b] *Allen Institute for Brain Science, Seattle, WA 98103, USA*

Received 24 May 2006
Available online 19 June 2006

Abstract

Ccd1, a DIX domain containing Zebrafish protein involved in neural patterning, is a positive regulator of the Wnt signaling pathway. DIXDC1, the human homolog of Ccd1, has two predominant isoforms. The short form (s-DIXDC1) has a similar amino acid sequence compared with Ccd1, while the long form (l-DIXDC1) contains an extra N-terminal sequence containing a calponin-homology (CH) domain, suggesting additional interaction with actin that we have performed detailed analysis in this report. We show that mRNA expression of both *DIXDC1* isoforms can be detected in various adult tissues by Northern blot analysis and is most abundant in cardiac and skeletal muscles. Both endogenous and ectopically expressed l-DIXDC1, but not s-DIXDC1, in cultured mammalian cells is localized to actin stress fibers at the filament ends in focal adhesion plaques. More importantly, l-DIXDC1 can directly bind to filamentous actin both *in vitro* and *in vivo* and the binding is mediated via a novel actin-binding domain (ABD) from amino acid 127 to 300. Thus, our data provide the first evidence that l-DIXDC1 may act as a novel branching component in the Wnt signaling pathway targeting both β-catenin–TCF complex for gene expression and cytoskeleton for regulating dynamics of actin filaments.

Keywords: DIXDC1; DIX domain; Actin-binding protein; Dvl; Wnt signaling

Actin cytoskeleton is essential for intracellular transport, cell motility, and morphology change. Dynamics of actin filaments are regulated *in vivo* by a plethora of actin-binding proteins (ABPs). ABPs can be classified into several functional groups [1], including monomer-binding proteins [2], filament-depolymerizing proteins [3], filament end-binding proteins [4], filament severing proteins [5], filament cross-linking proteins [6], filament stabilizing proteins [7], and motor proteins [8]. ABPs interact with monomeric actin (G-actin) or filamentous actin (F-actin) via actin-binding domains (ABDs). Most ABDs can be grouped into a few conserved families [9], one of which is called calponin-homology domain (CH domain). Not all proteins containing CH domains can actually bind actin and in most cases, a tandem repeat of CH domains is required to form a complete and functional ABD [10]. Unique actin-binding motifs also exist in some ABPs [11–14]. The DIX (DAX) is a key domain responsible for the interaction between Dvl and actin, and it targets Dvl to actin and vesicular membranes [13]. This unique structural and functional domain is present in Axins (Axin1 and Axin2) and Dvls (Dvl-1, Dvl-2, and Dvl-3), all of which are Wnt signaling pathway components [13,15,16]. The DIX domain in the Wnt signaling pathway is involved in both homo-oligomerization and hetero-oligomerization among Axins and Dvls in forming the multiprotein complex of APC, GSK-3, and β-cateinin to regulate T-cell-factor (TCF) signaling [17].

DIXDC1 is the human homolog of Ccd1, a recently identified novel DIX domain containing protein in Zebrafish [18,19]. It is a positive regulator in the Wnt signaling pathway functioning downstream of Wnt and upstream of Axin. Ccd1 also contains a coiled-coil domain (MTH domain) besides the DIX domain [20]. Like Dvl, full-length

* Corresponding author. Fax: +1 507 266 5193.
E-mail address: liu.wanguo@mayo.edu (W. Liu).

0006-291X/$ - see front matter © 2006 Elsevier Inc. All rights reserved.
doi:10.1016/j.bbrc.2006.06.050

Ccd1 activates T-cell-factor (TCF) signaling in a TCF reporter assay. However, deletion of either the MTH domain or the DIX domain abolished TCF activation. Overexpression of Ccd1 has been shown to reduce eye size and forebrain in zebrafish, and this phenotype is similar to those caused by overexpression of Wnt8 and its receptor in the same organism [18]. However, how Ccd1 positively regulates Wnt signaling and why overexpression of Ccd1 deregulates zebrafish neural patterning is not known. DIXDC1 protein has also been implicated as an inhibitor of Dvl- and Axin-mediated activation of the c-Jun N-terminal kinase (JNK) pathway [21]. Similar to TCF activation, both DIX and MTH domains of DIXDC1 are required for JNK activation through distinct mechanisms, indicating that DIXDC1 may play diverse roles in not only axis formation and neural patterning during embryonic development but also normal cell growth and differentiation.

We recently reported the identification of frameshift mutations in the *AXIN2* gene in more than 25% of colorectal cancers (CRC) with microsatellite instability (MSI) [22]. In an effort to understand why mutant AXIN2, which is completely depleted of its C-terminal DIX domain, is associated with CRC tumorigenesis, we isolated several proteins that interact with this C-terminal region of Axin2 and one of which is DIXDC1. We found that human DIXDC1 exists in different isoforms and one of the predominant isoforms is the long form (l-DIXDC1, GenBank Accession No. DQ642016), which has an extra N-terminal sequence containing a CH domain compared with Ccd1. In this study, we report that in fact l-DIXDC1 is a bona fide ABP at filament ends and identification of a novel ABD within its N-terminus. We suggest that l-DIXDC1 is a cytoskeletal-associated protein that may be involved in modulating dynamics of actin filaments.

Materials and methods

Northern blotting, 5′ RACE, and RT-PCR. MTN blot was purchased from BD Clontech. The 1.1 kb cDNA probe for detecting both human *l-DIXDC1* and *s-DIXDC1* mRNA at the same time was amplified by PCR using the following primer pair: 5′cccgaggaacaactgattat3′/5′aagcagccaggg agtgacc3′. A 595 bp *Nhe*I–*Apa*I DNA fragment encoding N-terminus of l-DIXDC1 was used to detect *l-DIXDC1* mRNA only. A specific cDNA probe for *s-DIXDC1* of 406 bp was generated by PCR using a primer pair within its exon 1 absent in *l-DIXDC1*: 5′ccagtgggagatgggttgagatgcc3′/5′cttgcgtccctcccatggtcc3′. The human β-actin cDNA control was purchased from Clontech. All the probes were labeled using Megaprime DNA Labeling Kit (Amersham) to more than 70% incorporation efficiency and directly used in hybridization at $2–4 \times 10^6$ cpm/ml without purification. The hybridization was performed in aqueous buffer at 68 °C overnight and washed with high stringency. The 5′ RACE was performed using total RNA isolated from HCT116 cell line and 5′ RACE System (Invitrogen). The primers used in the 5′ RACE are 5′tcaggcaggctagcattgttc3′, 5′ccagtaagttccctcgggtca3′, and 5′gcttcactgctggcctcttcttc3′. RT-PCR was performed using total RNA isolated from various cell lines and tissues as templates and Superscript™ II First-Strand Synthesis System for RT-PCR (Invitrogen).

Generation and purification of rabbit polyclonal antibody. Polypeptide from 567 to 589 amino acids of DIXDC1 was synthesized and conjugated to KLH at the Protein Core Facility at Mayo Clinic. Immunization of rabbits was completed and sera collected at Rockland Immunochemicals Inc. The polyclonal antibody (coded as AD2) was affinity-purified using the SulfoLink Kit (Pierce) according to manufacturer's instructions.

Cell culture, DNA expression constructs, and transient transfection. Saos-2 cells were cultured in McCoy5A medium supplemented with 15% FBS. HeLa, 293T, HCT116, and all other cell lines mentioned in the paper were cultured according to ATCC recommendations. FLAG-tagged l-DIXDC1, s-DIXDC1, l-DIXDC1 (ΔCH), l-DIXDC1 (ΔMTH), l-DIXDC1 (ΔDIX), HA- and Myc-tagged l-DIXDC1 were expressed in vector pCMV-tag2A (Stratagene). EGFP-FLAG-l-DIXDC1 fusion protein was expressed in pEGFP-C1 vector (Clontech). Transient transfections were performed either in 100-mm dishes or 7-mm HTC slides (Cell-line) using FuGENE 6 (Roche) as the transfection reagent according to manufacturer's instructions.

Western blot analysis, immunostaining, and immunoprecipitation. To immunoprecipitate the ectopically expressed protein, whole cell lysates were obtained using Beach lysis buffer: 50 mM Tris–HCl, pH 8.0, 150 mM NaCl, 15 mM $MgCl_2$, 5 mM EDTA, 1% NP-40, and protease inhibitor cocktail (Roche). After centrifugation at 15,000*g* at 4 °C for 15 min, the pellets were redissolved in Puri lysis buffer: 50 mM Tris–HCl, pH 8.0, 150 mM NaCl, 15 mM $MgCl_2$, 5 mM EDTA, 1% SDS with protease inhibitor cocktail, and subsequently 1:10 diluted with Beach lysis buffer. The diluted samples were then incubated with Easy-View gel conjugated with M2 antibody (Sigma) to pull down FLAG-tagged DIXDC1 as described by the manufacturer. The precipitated protein was resolved on 4–15% SDS–PAGE gels, transferred onto PVDF membrane (Bio-Rad) for Western blot analysis using the indicated antibodies, and visualized by ECL (Amersham).

Co-immunoprecipitation of Myc-l-DIXDC1 and β-actin was performed using the Immunoprecipitation Kit-Protein A (Roche) according to manufacturer's instructions. Briefly, HeLa cells transfected with Myc-l-DIXDC1 were lysed in lysis buffer (50 mM Tris–HCl, pH 7.5; 150 mM NaCl, 1% NP40, 0.5% sodium deoxycholate, and complete protease inhibitor cocktail) and immunoprecipitated with monoclonal anti-Myc antibody (9E10, Roche). Samples were washed four times with lysis buffer, eluted with Laemmli buffer, and resolved on SDS–PAGE. Immunoblot was performed with mouse monoclonal antibody against β-actin (AC-15, Sigma). Similarly, endogenous DIXDC1 was immunoprecipitated by rabbit anti-DIXDC1 antibody AD2.

For the immunostaining of the endogenous or epitope-tagged DIXDC1, cells were fixed with 3% paraformaldehyde in 1× PBS and permeabilized with 0.2% Triton X-100 at room temperature for 5 min. The cells were then blocked in 3% milk in 1× PBS and stained with primary antibodies. The antibodies used in primary staining are rabbit polyclonal antibody anti-DIXDC1 (AD2), mouse monoclonal antibody anti-FLAG (M2), anti-vinculin (hVIN-1), anti-Myc(9E10), and anti-HA (12CA5). Alexa Fluor 488 and 594 phalloidin, Alexa Fluor 594 goat anti-rabbit IgG antibody, Alexa Fluor 488, 594, and 680 goat anti-mouse IgG antibodies (Molecular Probes) were used in the secondary staining. The indirect immunofluorescence was visualized and recorded on a Carl Zeiss Confocal Laser Scanning Microscope LSM510.

Solubility and F-actin cosedimentation assays. For solubility assays, 293T cells were lysed in ice-cold lysis buffer: 50 mM Tris–HCl, 150 mM NaCl, 2.5 mM $MgCl_2$, 1 mM EDTA, and 1% NP-40 supplemented with protease inhibitor. The lysates were incubated on ice for 30 min, vortexed occasionally, and then centrifuged at 15,000*g* and 4 °C for 15 min. Fractions of supernatant and pellets were collected and redissolved in Laemmli sample buffer for SDS–PAGE. The proteins were detected by Western blot using anti-FLAG (M2) antibody.

For F-actin cosedimentation assays, FLAG-l-DIXDC1 bound to Easy-View gel was eluted using 100 mM glycine, pH 2.5, and neutralized with 1 M Tris–HCl, pH 9.6. GST-fusion protein of DIXDC1 was eluted from glutathione beads using 10 mM glutathione at pH 8.0. All the protein was then prespun at 100,000*g* at 4 °C for 30 min and the supernatant was used in the cosedimentation experiments based on manufacturer's protocol (Cytoskeleton, Denver, CO). Cosedimenting proteins were resolved on SDS–PAGE gels and visualized either by Coomassie blue staining or Western blot.

Interfering siRNA knockdown. Depletion of DIXDC1 was achieved via plasmid-based siRNA knockdown approach. The hairpin siRNA inserts were prepared by annealing two oligos and cloned into pSilencer 3.1-H1 (Ambion) via *Bam*HI and *Hin*dIII sites. The top and bottom strand sequences of *DIXDC1* siRNA#1 are 5′-GATCCAGAGCGAGTCCATT ATAACTTCAAGAGAGTTATAATGGACTCGCTCTTTTTTTG GAAA-3′ and 5′-AGCTTTTCCAAAAAAAGAGCGAGTCCATT ATAACTCTCTTGAAGTTATAATGGACTCGCTCTG-3′, and the sequences of siRNA#2 are 5′-GATCCGGATGCCTTGCAGCAGA GATTCAAGAGATCTCTGCTGCAAGGCATCCTTTTTTGGAA A-3′ and 5′-AGCTTTTCCAAAAAAGGATGCCTTGC AGCAGAGA TCTCTTGAATCTCTGCTGCAAGGCATCCG-3′. The HeLa cells were transfected for two consecutive times using the knockdown constructs via electroporation with an interval of 24 h and subjected to Western blot analysis 3 days after first transfection.

Results

Identification, tissue distribution, and alternative spliced forms of human DIXDC1

We previously cloned the *AXIN2* gene and showed that this gene is mutated in more than 25% of colorectal cancer (CRC) with microsatellite instability (MSI) and mutant Axin2 activates TCF activity, a hallmark of cancer development [16,22]. To determine why deletion of C-terminus of Axin2 is associated with tumorigenesis in CRC, we identified several AXIN2 C-terminal-binding proteins using AXIN2 (aa 655–843) as a bait in a yeast two-hybrid screen and one of the identified clones had the same sequence as DIXDC1 (data not shown). Northern blot analysis with a 1.1 kb *DIXDC1* probe, corresponding to the C-terminal half of the open reading frame (ORF) of the gene, showed *DIXDC1* to be ubiquitously expressed. Expression of *DIXDC1* was much more abundant in cardiac and skeletal muscles (Fig. 1A, panel C). At least four spliced variants of *DIXDC1* mRNA ranging in sizes from 5.1, 5.8, 6.3, and 6.8 kb were detected. Three different spliced products are present in cardiac and skeletal muscles (5.1, 6.3, and 6.8 kb), two in kidney and pancreas (5.8 and 6.3 kb), and all the other tissues have a common form (6.3 kb in brain, liver, lung, and placenta). We then performed 5′ RACE to investigate the 5′ UTR of different forms of *DIXDC1* mRNA from different tissues (cardiac and skeletal muscles, pancreas and colon tissues) and cultured cell lines (HeLa and HCT116). Two major forms with differential transcription initiation sites were identified encoding one long and one short protein product that we termed as l-DIXDC1 (GenBank Accession No. DQ642016) and s-DIXDC1 (DIXDC1 isoform b, [21]), respectively (Fig. 1B). The short form is a homolog of zebrafish Ccd1 while l-DIXDC1 has an extra N-terminal segment of 211 amino acids containing a calponin-homology (CH) domain (aa 21–128). We further confirmed the aforementioned results by RT-PCR analysis using unique primers for *l-DIXDC1* or *s-DIXDC1* (data not shown) and by Northern blot analysis using two different DNA probes specific for *l-DIXDC1* and *s-DIXDC1* (Fig. 1A, panels A and B). The 6.3 kb band shown in all tissues in panel C appears to represent the *l-DIXDC1*, while the 5.1 kb band which is abundant in cardiac and skeletal muscles is *s-DIXDC1*.

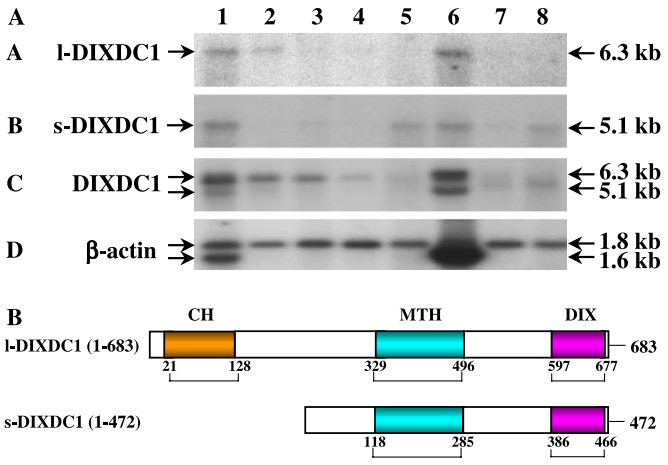

Fig. 1. DIXDC1 protein exists as two predominant isoforms. (A) Tissue distribution of human *DIXDC1* poly(A)$^+$ RNA by Northern blot analysis. The cDNA probes used in the Northern blot analysis were synthesized as described in Materials and methods. Lane 1, heart; lane 2, brain; lane 3, placenta; lane 4, lung; lane 5, liver; lane 6, skeletal muscle; lane 7, kidney, and lane 8, pancreas. Panel A, all *DIXDC1* isoforms; panel B, *l-DIXDC1*; panel C, *s-DIXDC1*; and D, human β-actin. (B) Domain structures of l-DIXDC1 and s-DIXDC1 proteins. CH, MTH, and DIX domains are shown.

During the preparation for this manuscript, Shiomi et al. reported the identification of various spliced forms for mouse Ccd1 [19]. Based on amino acid sequence similarities, l- and s-DIXDC1 corresponds to mouse AβL and BαL isoforms, the two predominant isoforms expressed in multiple mouse tissues, respectively. More importantly, Ccd1AβL, the mouse homolog of 1-DIXDC1, is predominantly expressed in various stages of mouse embryos indicating a potential role of this protein during early development.

Distinct pattern of subcellular localization of l- and s-DIXDC1

The CH and DIX domains present in DIXDC1 have been previously studied in other proteins and demonstrated to target actin-binding [10,13]. We used an indirect immunofluorescence technique to determine whether endogenous DIXDC1 is also associated with cytoskeleton in mammalian cells. A rabbit polyclonal antibody coded AD2 against polypeptide epitope aa 567–589 in DIXDC1 was generated and affinity-purified. The antibody was first tested by Western blot analysis of 293T cells with ectopic expression of FLAG-tagged l- and s-DIXDC1. As shown in Fig. 2A, antibody AD2 could recognize both proteins in the whole cell lysate. We then used AD2 for immunofluorescence staining of endogenous DIXDC1 in HeLa cells and Alexa Fluor 488 phalloidin to simultaneously visualize F-actin. Other than cytoplasmic staining presumed as s-DIXDC1, AD2 clearly stains the ends of actin stress

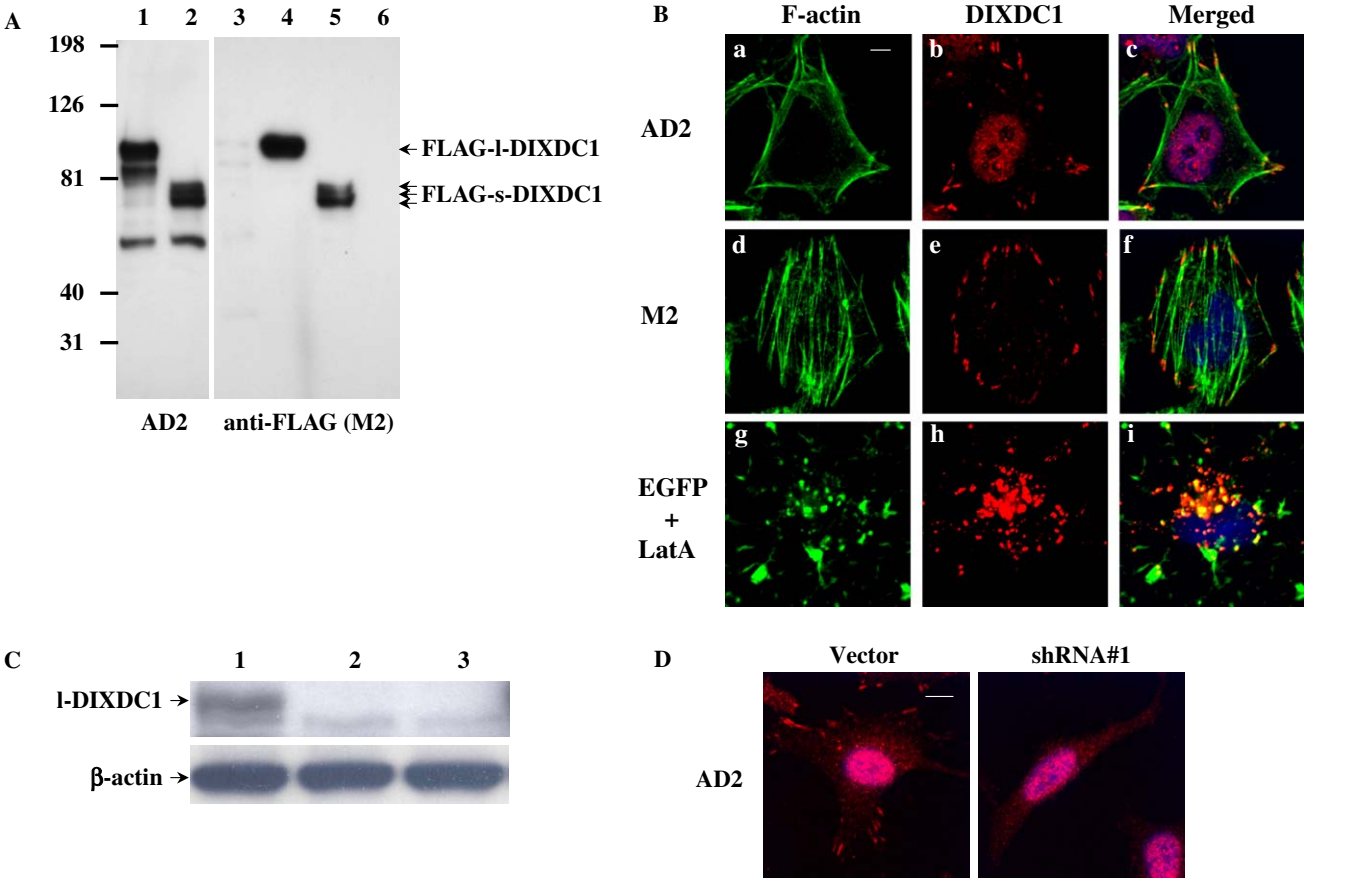

Fig. 2. Subcellular localization of endogenous and exogenous l-DIXDC1 at F-actin. (A) Western blot analysis of expression of FLAG-l-DIXDC1 and FLAG-s-DIXDC1 in 293T cells. Whole cell lysates of FLAG-l-DIXDC1 and FLAG-s-DIXDC1 were analyzed using purified rabbit polyclonal antibody AD2 (lanes 1 and 2). Triton-soluble (lanes 3 and 5) and Triton-insoluble (lanes 4 and 6) fractions of FLAG-l-DIXDC1 (lanes 3 and 4) and FLAG-s-DIXDC1 (lanes 5 and 6) were analyzed using mouse monoclonal anti-FLAG antibody M2. Three close bands were present for FLAG-s-DIXDC1 that might be due to post-translational modification such as phosphorylation. (B) The endogenous DIXDC1 in HeLa cells was stained with primary antibody AD2 and secondary Alexa Fluor 594 goat anti-rabbit IgG antibody (a–c). The ectopic expressed l-DIXDC1 was stained by anti-FLAG (M2) and Alexa Fluor 594 goat anti-mouse IgG antibodies in HeLa cells 24 h after being transfected with pCMV-tag2A-FLAG-l-DIXDC1 (d–f). Saos-2 cells with expression of EGFP-FLAG-l-DIXDC1 were treated with 1 μM Latrunculin A for 4 h before immunostaining (g–i). F-actin was labeled by Alexa Fluor 488 (a,d) or Alexa Fluor 594 phalloidin (g) and the nuclear DNA was stained by Hoechst dye. The images were taken on an LSM510 laser scanning microscope. The size bar (a) is 5 μm for all the images. (C) Western blot analysis of siRNA knockdown of l-DIXDC1 protein in HeLa cells. Lane 1, vector alone; 2, shRNA#1; 3, shRNA#2. (D) Significant reduction of l-DIXDC1 at the ends of filamentous actin in HeLa cells with siRNA knockdown. HeLa cells were transfected with shRNA#1 and immunostained by AD2 and Alexa Fluor 594 goat anti-rabbit IgG antibodies. HeLa cells transfected with pSilencer vector alone were used as controls. The size bar is 10 μm.

fibers proximal to the cellular membrane within the adhesion plaques (Fig. 2B, a–c). The same results were obtained using AD2 antibody to stain a variety of cell lines including DU145, HeLa, MCF7, SkBr3, Saos-2, and HCT116 (data not shown). The cellular localization of ectopic DIXDC1 was also determined by staining Saos-2 cells expressing FLAG-l-DIXDC1 with anti-FLAG antibody (M2) (Fig. 2B, d–f). In Saos-2 cells with low level expression, FLAG-l-DIXDC1 was initially seen at the ends of the stress fibers adjacent to cellular membranes resembling that observed for endogenous DIXDC1. In Saos2 cells with high-level expression, however, the staining of FLAG-l-DIXDC1 extended to all actin filaments. This pattern was also visualized in Saos-2 cells expressing EGFP-FLAG-l-DIXDC1 fusion protein (data not shown). In HeLa and 293 cells, ectopic expression of l-DIXDC1 in each individual cell is always very strong so that all actin filaments are positively stained (data not shown). Specificity of the immunostaining was further confirmed when the synthesized polypeptide 567–589 was used to successfully block the positive staining of l-DIXDC1 by AD2 (data not shown). Cellular distribution of EGFP-l-DIXDC1 in Saos2 cells was dramatically affected by Latrunculin A treatment that depolymerized actin cytoskeleton (Fig. 2B, g–i). Four hours after the addition of Latrunculin A, actin filaments were disrupted and EGFP-FLAG-l-DIXDC1 formed cytoplasmic aggregates close to the nucleus. Some of the aggregates still colocalized with actin suggesting that l-DIXDC1 remained physically associated with actin monomers.

The specificity of l-DIXDC1 staining at the F-actin tips was further confirmed by immunostaining analysis using hairpin siRNA targeting the coding region of DIXDC1. We developed two shRNAs cloned into pSilencer 3.1-H1

that were able to reduce ectopic expression of l-DIXDC1 by over 90% (data not shown). We then tested the effectiveness of these two siRNAs to deplete expression of endogenous l-DIXDC1 in HeLa cells by Western blot analysis. As shown in Fig. 2C, 3 days after the expression of both shRNAs, endogenous l-DIXDC1 was significantly reduced by at least 90% estimated by densitometry analysis. In the subsequent immunostaining experiment with shRNA#1, staining of l-DIXDC1 at the ends of actin filaments in HeLa cells was also eliminated (Fig. 2D). Therefore, l-DIXDC1 associates with actin cytoskeleton preferably at the ends of the filaments.

Since focal adhesions are specialized structures formed at the ends of filamentous actin, we used an anti-vinculin antibody (hVIN1) as a marker to see if l-DIXDC1 resides in these cellular assemblies. As expected, AD2 recognized endogenous DIXDC1 that colocalized with vinculin at focal adhesion plaques in Saos-2 cells (Fig. 3A–D). Similar to endogenous DIXDC1, the ectopically expressed FLAG-l-DIXDC1 and EGFP-l-DIXDC1 also overlapped with vinculin staining at the tips of F-actin (data not shown). Thus, both endogenous and exogenous l-DIXDC1 colocalize with vinculin in the focal adhesion complex. A higher magnification image of triple staining of DIXDC1, vinculin, and F-actin at focal adhesions reveals a subtle difference in spatial distribution of DIXDC1 and vinculin relative to F-actin (Fig. 3E–H). In most cases, l-DIXDC1 colocalized exactly with the ends of F-actin while staining of vinculin often extended from the tips of F-actin towards the edge of membrane. Since we were unable to co-immunoprecipitate vinculin with both exogenous and endogenous l-DIXDC1 in our experiments, the partial overlap of l-DIXDC1 and vinculin indicates that l-DIXDC1 may not directly bind to vinculin within focal adhesion complexes.

Direct interaction of l-DIXDC1 with actin filaments in vitro and in vivo

Association of l-DIXDC1 with actin was further revealed by co-immunoprecipitation of these two proteins. β-Actin could be immunoprecipitated with ectopically expressed Myc-l-DIXDC1 indicating that they associate with each other directly or indirectly in a protein complex (Fig. 4A). Furthermore, endogenous actin could also co-immunoprecipitate with endogenous DIXDC1 using AD2 antibody (Fig. 4B, panels A and B). Other than actin, myosin could also be pulled down together with DIXDC1 (Fig. 4B, panel C). To determine whether DIXDC1 directly binds to F-actin, we performed F-actin cosedimentation assay using immunoprecipitated FLAG-l-DIXDC1 and bacterially expressed GST-l-DIXDC1. Like α-actinin, FLAG-l-DIXDC1 cosedimented with purified F-actin, whereas the control BSA did not (Fig. 4C). The same held true for GST-l-DIXDC1, indicating that the cosedimentation resulted from a direct interaction between l-DIXDC1 and F-actin. Next we studied the kinetics of F-actin-binding by varying the concentrations of GST-l-DIXDC1 and calculated the binding constant K_d and saturation concentration B_{max} by means of non-linear regression analysis (Fig. 4D). K_d of GST-l-DIXDC1 bound to actin filaments is 0.03 μM, indicating a very strong and tight binding. The value of B_{max} is 0.025 μM, suggesting that 1 molecule of GST-l-DIXDC1 bound per 200 molecules of actin monomers (Fig. 4D).

A novel actin-binding domain from amino acid 127–300 targets l-DIXDC1 to actin filaments

To determine the exact ABD in l-DIXDC1, we performed cosedimentation assays using various GST-tagged

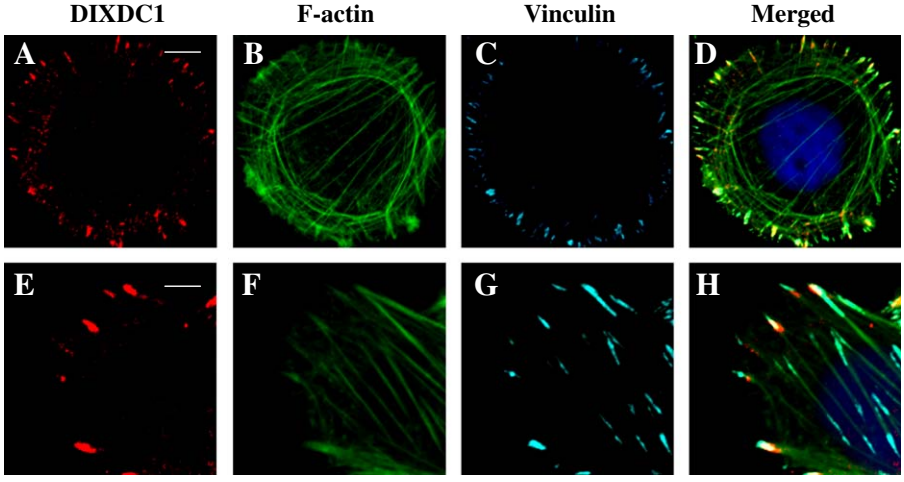

Fig. 3. Colocalization of l-DIXDC1 and vinculin at focal adhesion complex. The endogenous l-DIXDC1 was stained with primary antibody AD2 and Alexa Fluor 594 goat anti-rabbit IgG antibody (A,E). Actin filaments were labeled with Alexa Fluor 488 phalloidin (B,F). The endogenous vinculin was stained using the mouse monoclonal antibody hVIN-1 and Alexa Fluor 680 goat anti-mouse antibody (C,G) and the nuclear DNA was stained by Hoechst dye. The merged images (D,H) showed partial overlap of l-DIXDC1 and vinculin staining at the ends of F-actin. The size bar is 5 and 2 μm for the upper and lower panels, respectively.

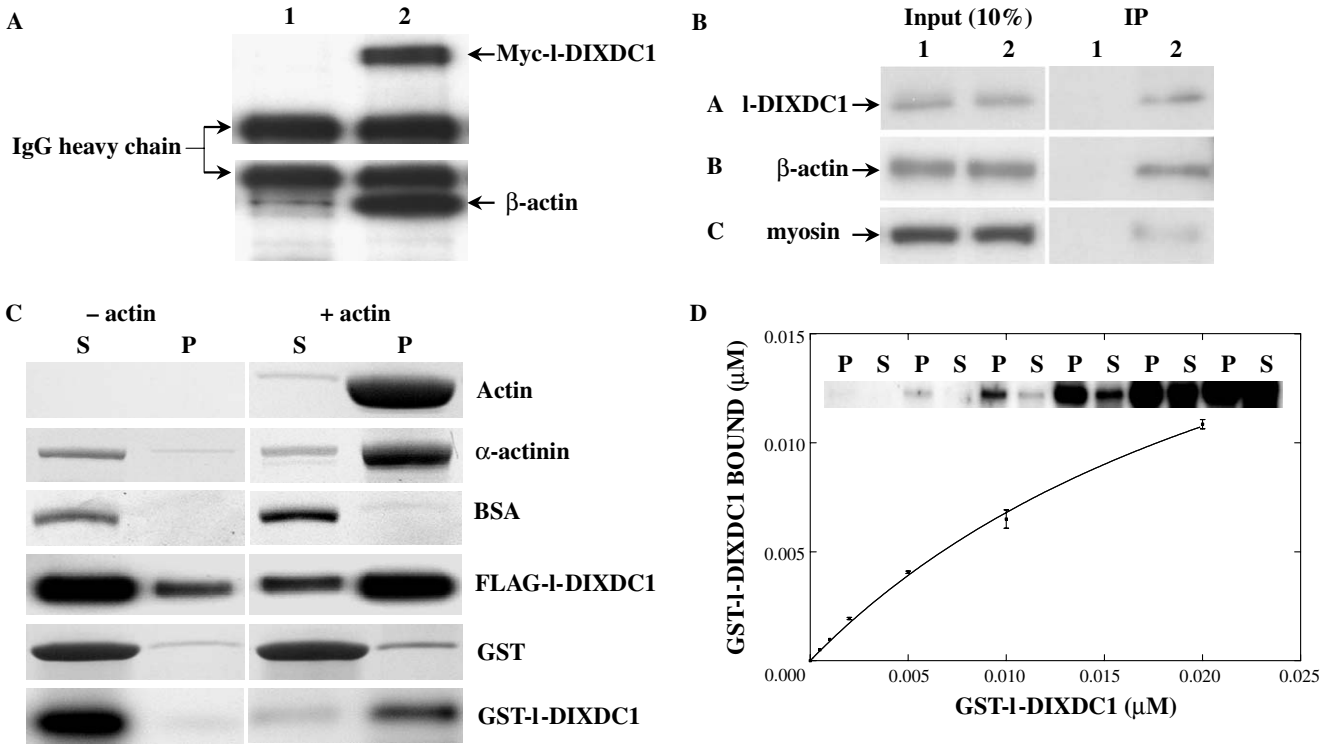

Fig. 4. Direct interaction of l-DIXDC1 with F-actin. (A) Co-immunoprecipitation of exogenous l-DIXDC1 with β-actin. The ectopic Myc-l-DIXDC1 was immunoprecipitated with mouse monoclonal anti-Myc (9E10), resolved by SDS-PAGE electrophoresis, and analyzed by Western blot analysis using mouse monoclonal anti-actin antibody. (B) Co-immunoprecipitation of endogenous l-DIXDC1 with β–actin and myosin. AD2 was used to immunoprecipitate l-DIXDC1 and actin and myosin were detected by mouse monoclonal anti-actin and rabbit anti-myosin (anti-myosin IIB (nonmuscle), Sigma) antibodies. (C) *In vitro* binding of recombinant l-DIXDC1 to F-actin. FLAG-l-DIXDC1 expressed in 293T cells was purified as described in the Materials and methods. GST-l-DIXDC1 was expressed in bacterial strain BL21 (DE3) and purified using the glutathione agarose beads. Binding of purified FLAG-l-DIXDC1 and GST-l-DIXDC1 were performed based on the manufacturer's instructions. BSA, α–actinin and GST were used as negative and positive controls, respectively. Actin, BSA, α-actinin, GST were stained by Commassie brilliant blue. FLAG-l-DIXDC1 and GST-l-DIXDC1 were shown by Western blot. (D) Kinetics of binding of GST-l-DIXDC1 to F-actin *in vitro*. Varied amounts of GST-l-DIXDC1 was incubated and then cosedimented with 5 μM F-actin. The amount of GST-l-DIXDC1 in supernatant and actin pellet was determined by Western blot and used to generate K_d and B_{max} values through non-linear regression analysis.

l-DIXDC1 deletion constructs. These analyses revealed that, to our surprise, a segment of amino acid from 127 to 300 between the CH and MTH domain is responsible for cosedimentation of GST-l-DIXDC1 with polymerized actin (Fig. 5A). We next expressed these variants with FLAG epitopes in 293T cells to test which variant could co-immunoprecipitate with endogenous actin. As shown in Fig. 5B, consistent with co-sedimentation results, all the variants containing the ABD domain (l-DIXDC1, ΔCH, ΔMTH, ΔDIX, and ABD) could precipitate actin while the variants lacking the domain (s-DIXDC1, ΔABD, and negative control) could not. The subcellular localization of these variants was further analyzed by indirect immunofluorescence. As shown in Fig. 5C, the ABD domain only (aa 127–300) could bind strongly to actin filaments (Fig. 5C, a–c). In contrast, s-DIXDC1 lacking the stretch of amino acid 1–219 present in l-DIXDC1 was in cytoplasm and did not associate with F-actin at all (Fig. 5C, d–f). The same held true for l-DIXDC1 with the ABD domain deleted (Fig. 5C, g–i). As it was also expected, deletion of the CH domain did not alter F-actin-binding by l-DIXDC1 (Fig. 5C, j–l). Although l-DIXDC1 with deletion of MTH or DIX domains showed a much more diffused staining pattern with a major portion of the expressed protein spreading all over the cytoplasm and concentrated in microspikes at the cell membranes, these variants still retained the ability to bind to actin stress fibers (Fig. 5C, m–r). Based on these data we conclude that tight and direct interaction of l-DIXDC1 with actin filaments is via a novel ABD from amino acid 127–300 in l-DIXDC1 (DIXDC1-ABD).

Discussion

In this study, we have provided strong evidence that l-DIXDC1 is an F-actin-binding protein. First, we showed colocalization of both endogenous and exogenous l-DIXDC1 with phalloidin-labeled actin filaments in all cell lines hitherto tested. It seemed in most cases that l-DIXDC1 is preferably associated with both ends of actin filaments. Second, we achieved co-immunoprecipitation of endogenous l-DIXDC1 with actin *in vivo* and we demonstrated cosedimentation of FLAG-l-DIXDC1 and GST-l-DIX-

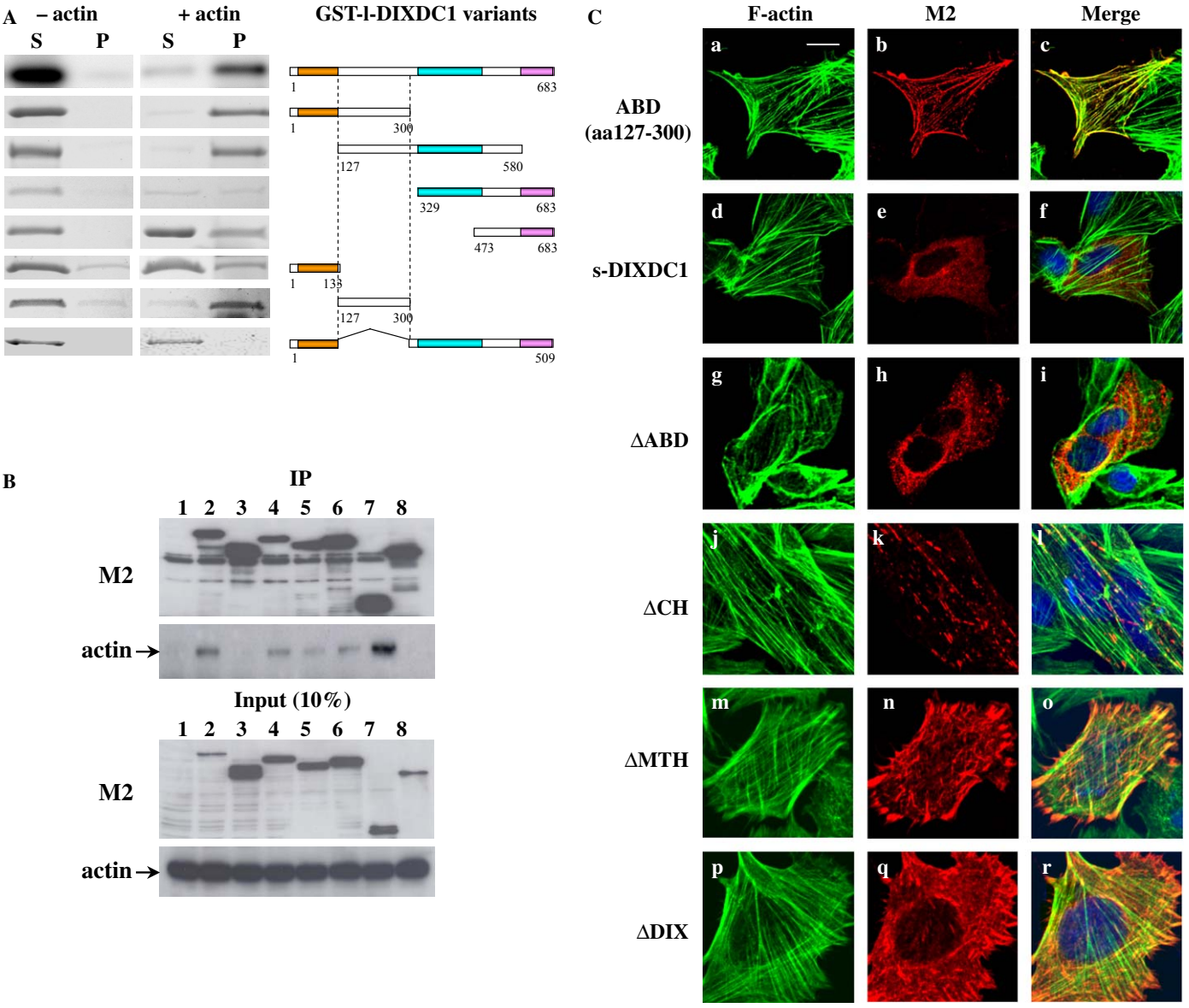

Fig. 5. Localization of a novel actin-binding domain (ABD) in l-DIXDC1. (A) Different regions of l-DIXDC1 were expressed as GST fusion proteins, purified and cosedimented with F-actin. Distribution of these GST fusion proteins in supernatant and pellet was examined by SDS–PAGE and Coomassie blue staining. (B) Co-immunoprecipitation of FLAG-tagged l-DIXDC1 variants with actin. Lane 1, mock; 2, l-DIXDC1; 3, s-DIXDC1; 4, l-DIXDC1-ΔCH; 5, l-DIXDC1-ΔMTH; 6, l-DIXDC1-ΔDIX; 7, l-DIXDC1-ABD; 8, l-DIXDC1-ΔABD. (C) *In vivo* association of FLAG-l-DIXDC1 with F-actin is mediated via the same ABD. Saos-2 cells were transfected with various constructs expressing FLAG-tagged wild-type and mutant l-DIXDC1 protein and immunostained with anti-FLAG (M2) and Alexa Fluor 594 goat anti-mouse IgG antibodies. Actin filaments were stained with Alexa Fluor 488 phalloidin. The size bar (a) is 10 μm for all images.

DC1 with F-actin *in vitro*. Third, we defined a novel motif DIXDC1-ABD (aa 127–300) required for actin-binding. Capelluto et al. have shown that DIX domain in Dvl2 could target the Wnt signaling protein to F-actin-binding [13]. Although DIX-deleted l-DIXDC1 was diffusely distributed in the cell, it still colocalized with phalloidin-labeled actin fibers (Fig. 5C, p-r) and it could still co-immunoprecipitate or co-sediment with actin (Fig. 5A and B). Moreover, FLAG-s-DIXDC1 with DIX domain did not colocalize with F-actin *in vivo* (Fig. 5C, d–f) and could not co-immunoprecipitate or cosediment with actin (Fig. 5A and B). These data strongly indicate that F-actin binding of l-DIXDC1 is not mediated via its DIX domain. Our data also showed that the single CH domain in l-DIXDC1 (aa 21–126) is not an ABD for l-DIXDC1, which is in agreement with current hypothesis that only CH domains in tandem repeat can actually bind to actin [10]. In conclusion, DIXDC1-ABD is sufficient and necessary for l-DIXDC1 to interact with F-actin both *in vitro* and *in vivo*. DIXDC1-ABD bears no significant sequence similarities to any conserved or unique ABDs that have been identified in various ABPs [1,11–14]. Thus, further refinement of the

domain and delineation of those amino acids that are crucial for F-actin-binding remain to be investigated.

F-actin-binding capability and subcellular localization at focal adhesions of l-DIXDC1 are reminiscent of another Wnt signaling pathway protein Dvl [13,23]. Full-length Dvl protein activates canonical Wnt signaling and stabilizes cytosolic β-catenin by translocating to the membranous structures [17]. In the planar cell polarity (PCP) pathway, Dvl regulates cytoskeletal reorganization and cell morphogenesis by targeting to the actin stress fibers and focal adhesion plaques [13]. Dvl-2 also mediates Wnt3a-induced cell motility and spreading that requires RhoA activation [24]. Recently, it has been shown that Dvl can heterodimerize with Ccd1 via their DIX domains [18]. In our experiments, l-DIXDC1 could also bind to Dvl2 via its DIX domain and these two proteins could colocalize to actin stress fibers when overexpressed (data not shown). These data implicate that l-DIXDC1 and Dvl may act in association at the same branching site in both canonical and non-canonical pathways [19]. However, there are apparent structural, as well as functional, differences between these two signaling proteins. First, although they both have an evolutionarily conserved DIX domain, the functional implications of their DIX domains are different. Other than homo- and hetero-dimerization, Dvl DIX is responsible for binding to actin stress fibers and vesicular membranes while l-DIXDC1 associates with F-actin via its novel actin-binding motif. Second, Dvl has a well-characterized PDZ domain that binds to Frizzled receptor, Dapper, and Frodo mediating canonical Wnt signaling [25]; on the other hand, however, MTH and DIX domains are required for TCF activity of mouse Dixdc1 in the presence of Dvl [19] and human DIXDC1 in our own luciferase reporter gene assays (data not shown). Third, in non-canonical Wnt pathway, Dvl regulates JNK signaling pathway essentially via its DEP domain [25]. However, it has recently been shown that coiled-coil DIX1 (s-DIXDC1) inhibits JNK pathway activation mediated by Axin1 and Dvl2 protein [21]. Therefore, future studies should focus on dissecting the diverse and unique roles of DIXDC1, in association with Dvl, in both canonical and non-canonical Wnt signaling pathways.

Acknowledgments

We thank Dr. Mark A. McNiven and Dr. Daniel D. Billadeau for helpful discussions and constructive criticism. This work was supported by Mayo Clinic/Foundation.

References

[1] C.G. dos Remedios, D. Chhabra, M. Kekic, I.V. Dedova, M. Tsubakihara, D.A. Berry, N.J. Nosworthy, Actin-binding proteins: regulation of cytoskeletal microfilaments, Physiol. Rev. 83 (2003) 433–473.

[2] V.O. Paavilainen, E. Bertling, S. Falck, P. Lappalainen, Regulation of cytoskeletal dynamics by actin-monomer-binding proteins, Trends Cell Biol. 14 (2004) 386–394.

[3] S. Ono, Regulation of actin filament dynamics by actin depolymerizing factor/cofilin and actin-interacting protein 1: new blades for twisted filaments, Biochemistry 42 (2003) 13363–13370.

[4] J.A. Cooper, D.A. Schafer, Control of actin assembly and disassembly at filament ends, Curr. Opin. Cell Biol. 12 (2000) 97–103.

[5] J.L. McGrath, E.A. Osborn, Y.S. Tardy, C.F. Dewey Jr., J.H. Hartwig, Regulation of the actin cycle in vivo by actin filament severing, Proc. Natl. Acad. Sci. USA 97 (2000) 6532–6537.

[6] R. Furukawa, M. Fechheimer, The structure, function, and assembly of actin filament bundles, Int. Rev. Cytol. 175 (1997) 29–90.

[7] P.W. Gunning, G. Schevzov, A.J. Kee, E.C. Hardeman, Tropomyosin isoforms: divining rods for actin cytoskeleton function, Trends Cell Biol. 15 (2005) 333–341.

[8] G. Kalhammer, M. Bahler, Unconventional myosins, Essays Biochem. 35 (2000) 33–42.

[9] R. Dominguez, Actin-binding proteins—a unifying hypothesis, Trends Biochem. Sci. 29 (2004) 572–578.

[10] M. Gimona, K. Djinovic-Carugo, W.J. Kranewitter, S.J. Winder, Functional plasticity of CH domains, FEBS Lett. 513 (2002) 98–106.

[11] D.L. Rimm, E.R. Koslov, P. Kebriaei, C.D. Cianci, J.S. Morrow, Alpha 1(E)-catenin is an actin-binding and -bundling protein mediating the attachment of F-actin to the membrane adhesion complex, Proc. Natl. Acad. Sci. USA 92 (1995) 8813–8817.

[12] Y. Isogawa, T. Kon, T. Inoue, R. Ohkura, H. Yamakawa, O. Ohara, K. Sutoh, The N-terminal domain of MYO18A has an ATP-insensitive actin-binding site, Biochemistry 44 (2005) 6190–6196.

[13] D.G. Capelluto, T.G. Kutateladze, R. Habas, C.V. Finkielstein, X. He, M. Overduin, The DIX domain targets dishevelled to actin stress fibers and vesicular membranes, Nature 419 (2002) 726–729.

[14] D. Pacholsky, P. Vakeel, M. Himmel, T. Lowe, T. Stradal, K. Rottner, D.O. Furst, P.F. van der Ven, Xin repeats define a novel actin-binding motif, J. Cell Sci. 117 (2004) 5257–5268.

[15] L. Zeng, F. Fagotto, T. Zhang, W. Hsu, T.J. Vasicek, W.L. Perry III, J.J. Lee, S.M. Tilghman, B.M. Gumbiner, F. Costantini, The mouse Fused locus encodes Axin, an inhibitor of the Wnt signaling pathway that regulates embryonic axis formation, Cell 90 (1997) 181–192.

[16] M. Mai, C. Qian, A. Yokomizo, D.I. Smith, W. Liu, Cloning of the human homolog of conductin (AXIN2), a gene mapping to chromosome 17q23-q24, Genomics 55 (1999) 341–344.

[17] S. Kishida, H. Yamamoto, S. Hino, S. Ikeda, M. Kishida, A. Kikuchi, DIX domains of Dvl and axin are necessary for protein interactions and their ability to regulate beta-catenin stability, Mol. Cell. Biol. 19 (1999) 4414–4422.

[18] K. Shiomi, H. Uchida, K. Keino-Masu, M. Masu, Ccd1, a novel protein with a DIX domain, is a positive regulator in the Wnt signaling during zebrafish neural patterning, Curr. Biol. 13 (2003) 73–77.

[19] K. Shiomi, M. Kanemoto, K. Keino-Masu, S. Yoshida, K. Soma, M. Masu, Identification and differential expression of multiple isoforms of mouse coiled-coil-DIX1 (Ccd1), a positive regulator of Wnt signaling, Brain Res. Mol. Brain Res. 135 (2005) 169–180.

[20] M. Katoh, M. Katoh, KIAA1735 gene on human chromosome 11q23.1 encodes a novel protein with myosin-tail homologous domain and C-terminal DIX domain, Int. J. Oncol. 23 (2003) 145–150.

[21] C.K. Wong, W. Luo, Y. Deng, H. Zou, Z. Ye, S.C. Lin, The DIX domain protein coiled-coil-DIX1 inhibits c-Jun N-terminal kinase activation by Axin and dishevelled through distinct mechanisms, J. Biol. Chem. 279 (2004) 39366–39373.

[22] W. Liu, X. Dong, M. Mai, R.S. Seelan, K. Taniguchi, K.K. Krishnadath, K.C. Halling, J.M. Cunningham, L.A. Boardman, C. Qian, E. Christensen, S.S. Schmidt, P.C. Roche, D.I. Smith, S.N. Thibodeau, Mutations in AXIN2 cause colorectal cancer with

defective mismatch repair by activating beta-catenin/TCF signaling, Nat. Genet. 26 (2000) 146–147.
[23] M.A. Torres, W.J. Nelson, Colocalization and redistribution of dishevelled and actin during Wnt-induced mesenchymal morphogenesis, J. Cell Biol. 149 (2000) 1433–1442.
[24] Y. Endo, V. Wolf, K. Muraiso, K. Kamijo, L. Soon, A. Uren, M. Barshishat-Kupper, J.S. Rubin, Wnt-3a-dependent cell motility involves RhoA activation and is specifically regulated by dishevelled-2, J. Biol. Chem. 280 (2005) 777–786.
[25] H.C. Wong, A. Bourdelas, A. Krauss, H.J. Lee, Y. Shao, D. Wu, M. Mlodzik, D.L. Shi, J. Zheng, Direct binding of the PDZ domain of Dishevelled to a conserved internal sequence in the C-terminal region of Frizzled, Mol. Cell 12 (2003) 1251–1260.